Journal of Applied Mechanics and Technical Physics, Vol. 42, No. 4, pp. 665–671, 2001

EFFECT OF THE CHEMICAL REACTION AND INJECTION ON FLOW CHARACTERISTICS IN AN UNSTEADY UPWARD MOTION OF AN ISOTHERMAL PLATE

R. Muthucumaraswamy[1] and P. Ganesan[2]

UDC 532.72;669.015.23

The transient incompressible viscous fluid flow regime past a semi-infinite isothermal plate under conditions of natural convection is studied numerically. The solution obtained takes into account the first-order homogeneous chemical reaction and the mass flux through the plate. The calculated velocity profile is in good agreement with the known exact solution. Velocity, temperature, and concentration profiles are presented. It is shown that the fluid velocity decreases with increasing chemical reaction parameter. The distributions of local and averaged values of skin friction and Nusselt and Sherwood numbers are analyzed.

Introduction. There are some natural and industrial processes in which heat and mass transfer is a consequence of buoyancy effects caused by diffusion of heat and chemical species. The study of such processes is useful for improving a number of chemical technologies, such as fiber drawing, crystal pulling from the melt, and polymer production.

Stokes [1] obtained the exact solution of the Navier–Stokes equation for the incompressible viscous fluid flow past an impulsively started infinite horizontal plate. Following the analysis of [1], Soundalgekar [2] found the exact solution of the problem of the viscous flow past an impulsively started infinite isothermal vertical plate. A similar problem for the case of the flow past an infinite isothermal vertical plate with mass transfer was solved in [3]. In [4], this problem was analyzed numerically; the plate was assumed to be semi-infinite, and the governing equations (in a dimensionless form) were solved by an implicit finite-difference scheme of the Crank–Nicholson type. The mass-transfer process in an unsteady flow past an infinite isothermal vertical plate with homogeneous mass injection was analyzed in [5, 6] using the conventional technique of the Laplace transform. Das et al. [6] studied the effect of the first-order homogeneous chemical reaction on the process of an unsteady flow past an infinite vertical plate with a constant heat and mass transfer.

Nevertheless, the problem of unsteady natural convection near a semi-infinite vertical plate with regard for the chemical reaction has not been adequately studied. In the present work, this problem is solved using the implicit finite-difference Crank–Nicholson scheme.

1. Governing Equation and Mathematical Formulation. We consider an incompressible viscous fluid flow past an impulsively started semi-infinite isothermal vertical plate with mass addition. It is assumed that the influence of viscous dissipation in the energy equation is negligibly small, and there is a chemical reaction between the diffusing components and the fluid. The x axis is directed vertically upward along the semi-infinite plate, and the y axis is normal to the plate. Initially, the plate and the fluid have an identical temperature, and the concentration is homogeneous. At $t' > 0$, the plate starts to move vertically upward with a constant velocity u_0 in the direction opposite to the gravitational field. As a result of the first-order homogeneous chemical reaction, the temperature and concentration of reaction products near the plate increase.

Taking into account the above assumptions, the unsteady flow past a semi-infinite vertical plate is described by the following equations:

[1]Sri Venkateswara College of Engineering, Sriperumbudur 602105, India. [2]Anna University, Chennai 600025, India. Translated from Prikladnaya Mekhanika i Tekhnicheskaya Fizika, Vol. 42, No. 4, pp. 119–126, July–August, 2001. Original article submitted November 10, 1999; revision submitted January 20, 2001.

0021-8944/01/4204-0665 $25.00

$$\frac{\partial u}{\partial x}+\frac{\partial v}{\partial y}=0, \quad \frac{\partial u}{\partial t'}+u\,\frac{\partial u}{\partial x}+v\,\frac{\partial u}{\partial y}=g\beta(T'-T'_\infty)+g\beta^*(C'-C'_\infty)+\nu\,\frac{\partial^2 u}{\partial y^2},$$
$$\frac{\partial T'}{\partial t'}+u\,\frac{\partial T'}{\partial x}+v\,\frac{\partial T'}{\partial y}=\alpha\,\frac{\partial^2 T'}{\partial y^2}, \qquad \frac{\partial C'}{\partial t'}+u\,\frac{\partial C'}{\partial x}+v\,\frac{\partial C'}{\partial y}=D\,\frac{\partial^2 C'}{\partial y^2}-K_l C'. \tag{1}$$

The initial and boundary conditions are

$$\begin{aligned}
&t'\leqslant 0: \quad u=0, \quad v=0, \quad T'=T'_\infty, \quad C'=C'_\infty,\\
&t'>0: \quad u=u_0, \quad v=0, \quad T'=T'_w, \quad \frac{\partial C'}{\partial y}=-\frac{j''}{D} \quad \text{for} \quad y=0,\\
&\qquad\quad u=0, \quad T'=T'_\infty, \quad C'=C'_\infty \quad \text{for} \quad x=0,\\
&\qquad\quad u\to 0, \quad T'\to T'_\infty, \quad C'\to C'_\infty \quad \text{for} \quad y\to\infty.
\end{aligned}$$

By introducing the dimensionless quantities

$$X=\frac{xu_0}{\nu}, \quad Y=\frac{yu_0}{\nu}, \quad U=\frac{u}{u_0}, \quad V=\frac{v}{u_0}, \quad t=\frac{t'u_0^2}{\nu},$$
$$T=\frac{T'-T'_\infty}{T'_w-T'_\infty}, \quad \mathrm{Gr}=\frac{\nu g\beta(T'_w-T'_\infty)}{u_0^3}, \quad C=\frac{C'-C'_\infty}{j''\nu/(Du_0)}, \quad \mathrm{Gc}=\frac{g\beta^*\nu^2 j''}{Du_0^4},$$
$$\mathrm{Pr}=\frac{\nu}{\alpha}, \qquad \mathrm{Sc}=\frac{\nu}{D}, \qquad K=\frac{\nu K_l}{u_0^2},$$

system (1) is reduced to the following form:

$$\frac{\partial U}{\partial X}+\frac{\partial V}{\partial Y}=0, \qquad \frac{\partial U}{\partial t}+U\,\frac{\partial U}{\partial X}+V\,\frac{\partial U}{\partial Y}=\mathrm{Gr}\,T+\mathrm{Gc}\,C+\frac{\partial^2 U}{\partial Y^2},$$
$$\frac{\partial T}{\partial t}+U\,\frac{\partial T}{\partial X}+V\,\frac{\partial T}{\partial Y}=\frac{1}{\mathrm{Pr}}\,\frac{\partial^2 T}{\partial Y^2}, \qquad \frac{\partial C}{\partial t}+U\,\frac{\partial C}{\partial X}+V\,\frac{\partial C}{\partial Y}=\frac{1}{\mathrm{Sc}}\,\frac{\partial^2 C}{\partial Y^2}-KC. \tag{2}$$

The corresponding initial and boundary conditions are

$$\begin{aligned}
&t\leqslant 0: \quad U=0, \quad V=0, \quad T=0, \quad C=0,\\
&t>0: \quad U=1, \quad V=0, \quad T=1, \quad \frac{\partial C}{\partial Y}=-1 \quad \text{for} \quad Y=0,\\
&\qquad\quad U=0, \quad T=0, \quad C=0 \quad \text{for} \quad X=0,\\
&\qquad\quad U\to 0, \quad T\to 0, \quad C\to 0 \quad \text{for} \quad Y\to\infty.
\end{aligned} \tag{3}$$

2. Procedure of the Solution. The unsteady nonlinear coupled equations (2) with conditions (3) are solved using the implicit finite-difference Crank–Nicholson scheme.

We consider a rectangular domain of integration with the sides $X_{\max}=1$ and $Y_{\max}=16$, where $Y_{\max}$ corresponds to $Y=\infty$. The value $Y_{\max}$ lies well outside the boundary layers (dynamic, thermal, and concentration ones) and was chosen after preliminary calculations so that two last boundary conditions (3) were satisfied within the tolerance limit of 10^{-5}. After experimenting with several meshes, the mesh size was chosen equal to $\Delta X=0.05$ and $\Delta Y=0.25$, and the time step was $\Delta t=0.01$.

The calculations are performed until the steady state is reached. It is assumed that the steady solution is obtained when the difference in the values of U, and also the temperature T and concentration C, in two sequential time steps becomes smaller than 10^{-5} at all point of the mesh.

The local "truncation" error $O(\Delta t^2+\Delta Y^2+\Delta X)$ tends to zero when Δt, ΔX, and ΔY tend to zero. Hence, the scheme is compatible. The finite-difference scheme is unconditionally stable, as is shown in [4]. Stability and compatibility ensure convergence.

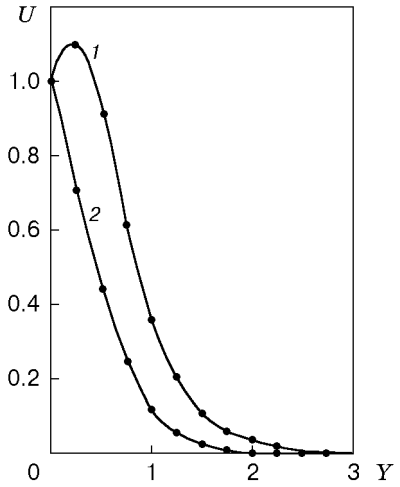

Fig. 1

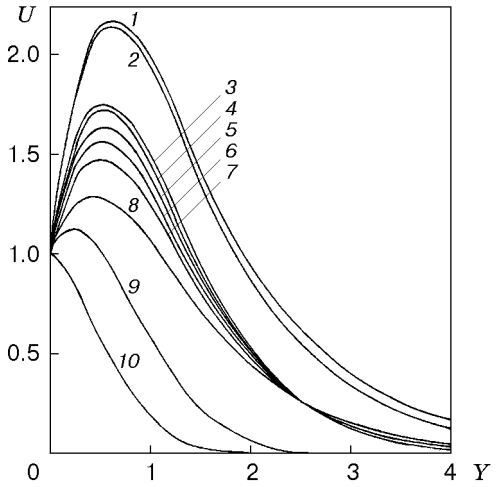

Fig. 2

Fig. 1. Velocity profiles in the absence of the reaction (Pr = 0.71, $t = 0.2$, and $K = 0$): the solid curves are the results of the present work and the points are the data of [5]; curve 1 refers to Gr = 5, Gc = 5, and Sc = 0.24 and curve 2 refers to Gr = 0.4, Gc = 0.2, and Sc = 1.

Fig. 2. Transient velocity profiles for $X = 1$ (Gr = 2, Gc = 5, and Pr = 0.71): curve 1 refers to $K = 0.2$, Sc = 0.16, and $t = 0.78$, curve 2 to $K = 0.2$, Sc = 0.16, and $t = 4.2$ (steady regime), curve 3 to $K = -2$, Sc = 0.6, and $t = 0.82$, curve 4 to $K = -2$, Sc = 0.6, and $t = 6.1$ (steady regime), curve 5 to $K = -1$, Sc = 0.6, and $t = 6.7$ (steady regime), curve 6 to $K = 0.2$, Sc = 0.6, and $t = 11.6$ (steady regime), curve 7 to $K = 2$, Sc = 0.6, and $t = 12.7$ (steady regime), curve 8 to $K = 0.2$, Sc = 2, and $t = 13.7$ (steady regime); curve 9 to $K = -2$, Sc = 0.6, and $t = 0.3$, and curve 10 to $K = -2$, Sc = 0.6, and $t = 0.15$.

3. Results and Discussion. To ascertain the accuracy of calculations, the data of the present study are compared with the known exact solution [5] for the case $K = 0$. The results compared are in good agreement (Fig. 1). The values $K > 0$ and $K < 0$ refer to destructive and generative reactions, respectively.

The transient velocity profiles are plotted in Fig. 2 for different values of the chemical reaction parameter and Schmidt numbers (cross section $X = 1$). It is seen that the velocity increases with time for Pr = 0.71, Gr = 2, Gc = 5, Sc = 0.6, and $K = -2$, reaches a maximum at $t = 0.82$, and becomes steady at $t = 6.1$. The velocity increases during the generative reaction and decreases during the destructive reaction. Obviously, the velocity increases with decreasing Schmidt number or chemical reaction parameter. The increase in velocity may be attributed to the fact that the rate of mass transfer in the fluid, which affects the buoyancy forces, increases as the Schmidt number decreases. The time necessary for the velocity to reach the steady state increases with increasing Schmidt number or chemical reaction parameter. However, the time needed to reach the steady velocity depends both on the Schmidt number and on the chemical reaction parameter. The contribution of mass diffusion to the buoyancy forces increases the maximum velocity significantly. Figure 3 shows the steady velocity profiles for different values of the thermal and mass Grashof numbers and the Prandtl number. The velocity increases with increasing thermal or mass Grashof number and decreases with increasing Prandtl number.

The transient and steady temperature profiles for different values of the Prandtl number and chemical reaction parameter are shown in Fig. 4. It is known that the Prandtl number plays an important role in flow processes, since it characterizes the ratio of thicknesses of the dynamic and thermal boundary layers. The temperature increases with increasing chemical reaction parameter and decreases with increasing Prandtl number.

The effect of the chemical reaction parameter and the Schmidt number is very important for concentration profiles. The transient and steady profiles of concentration for different values of the chemical reaction parameter are shown in Fig. 5. A decrease in concentration is observed with increasing chemical reaction parameter. Figure 6 shows the concentration profiles for different values of the thermal Grashof number. The concentration increases with decreasing Gr.

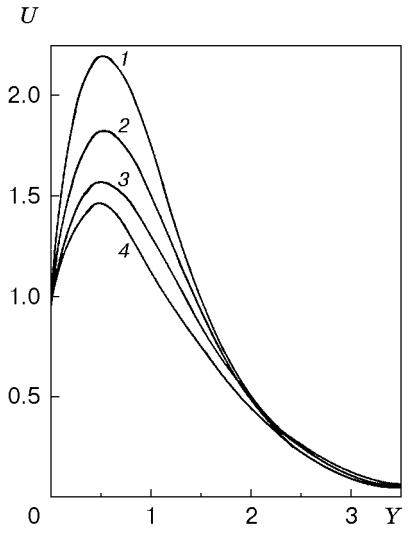

Fig. 3

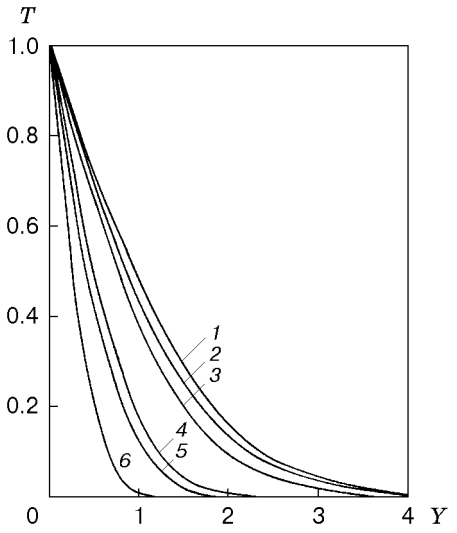

Fig. 4

Fig. 3. Steady velocity profiles for $X = 1$ (Sc = 0.6 and $K = 0.2$): curve 1 refers to Gr = 5, Gc = 10, Pr = 0.71, and $t = 7.1$, curve 2 to Gr = 5, Gc = 5, Pr = 0.71, and $t = 7.4$, curve 3 to Gr = 2, Gc = 5, Pr = 0.71, and $t = 11.6$, and curve 4 to Gr = 2, Gc = 5, Pr = 7, and $t = 10.3$.

Fig. 4. Temperature profiles for $X = 1$ (Gr = 2 and Gc = 5): curve 1 refers to $K = 2$, Pr = 0.71, and $t = 0.67$, curve 2 to $K = 2$, Pr = 0.71, and $t = 12.7$ (steady regime), curve 3 to $K = -2$, Pr = 0.71, and $t = 6.1$, curve 4 to $K = 2$, Pr = 0.71, and $t = 0.2$, curve 5 to $K = 2$, Pr = 0.71, and $t = 0.15$, and curve 6 to $K = 2$, Pr = 7, and $t = 10.4$ (steady regime).

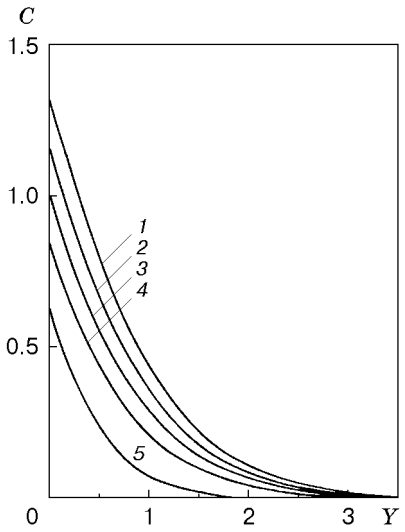

Fig. 5

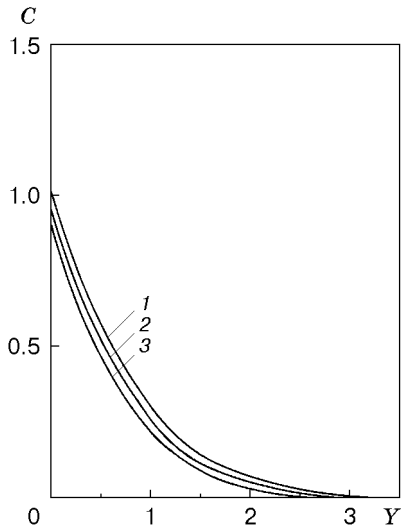

Fig. 6

Fig. 5. Concentration profiles for $X = 1$ (Gr = 2, Gc = 5, and Pr = 0.71): curve 1 refers to $K = -2$, Sc = 0.6, and $t = 6.1$, curve 2 to $K = -1$, Sc = 0.6, and $t = 6.7$, curve 3 to $K = 0.2$, Sc = 0.6, and $t = 11.6$, curve 4 to $K = 2$, Sc = 0.6, and $t = 12.7$, and curve 5 to $K = 0.2$, Sc = 2, and $t = 13.7$.

Fig. 6. Concentration profiles for $X = 1$ (Pr = 0.71, Sc = 0.6, $K = 0.2$, and Gc = 5) and Gr = 2 (1), 5 (2), and 10 (3).

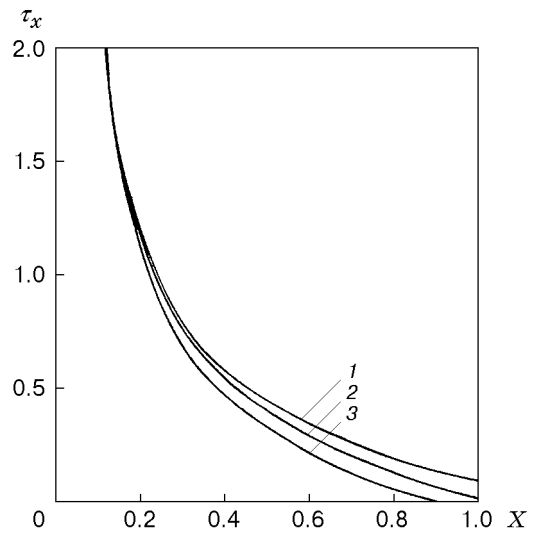

Fig. 7

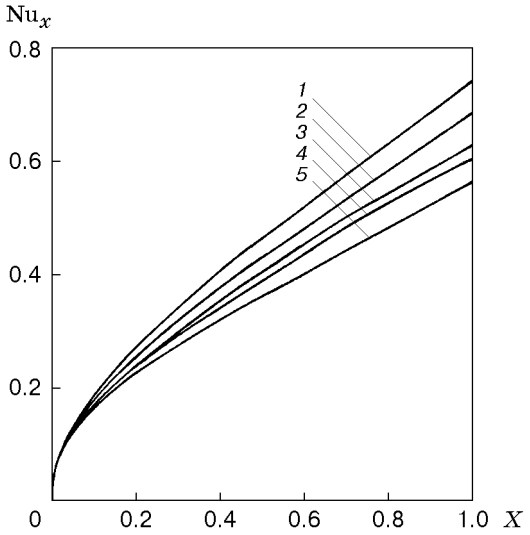

Fig. 8

Fig. 7. Local skin friction versus the coordinate X (Pr = 0.71, Gr = 0.4, and Gc = 0.2): curve 1 refers to $K = 0.2$ and Sc = 0.6, curve 2 to $K = -2$ and Sc = 0.6, and curve 3 to $K = 0.2$ and Sc = 0.16.

Fig. 8. Local Nusselt number versus the coordinate X (Pr = 0.71): curve 1 refers to Gr = 5, Gc = 10, Sc = 0.6, and $K = 0.2$, curve 2 to Gr = 5, Gc = 5, Sc = 0.6, and $K = 0.2$, curve 3 Gr = 2, Gc = 5, Sc = 0.6, and $K = 0.2$, curve 4 to Gr = 2, Gc = 5, Sc = 0.6, and $K = 2$, and curve 5 to Gr = 2, Gc = 5, Sc = 2, and $K = 0.2$.

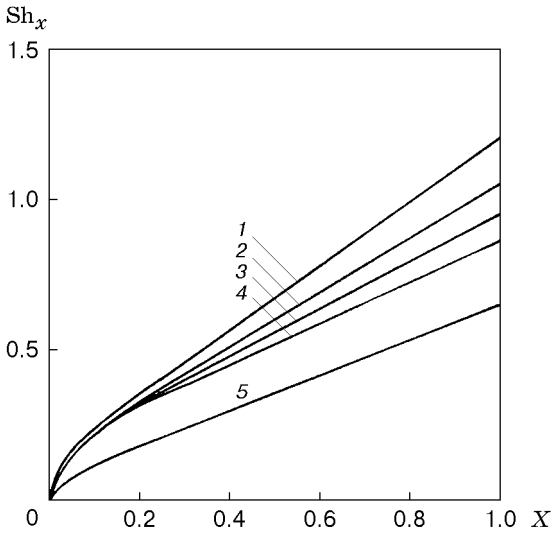

Fig. 9

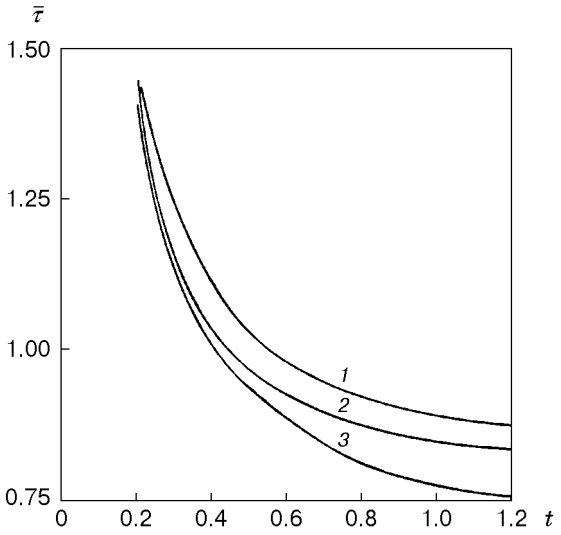

Fig. 10

Fig. 9. Local Sherwood number versus the coordinate X (Gr = 2, Gc = 5, and Pr = 0.71): curve 1 refers to $K = 2$ and Sc = 0.6, curve 2 to $K = 0.2$ and Sc = 0.6, curve 3 to $K = -1$ and Sc = 0.6, curve 4 to $K = -2$ and Sc = 0.6, and curve 5 to $K = 0.2$ and Sc = 0.16.

Fig. 10. Averaged skin friction versus time (Pr = 0.71, Gr = 0.4, and Gc = 0.2): curve 1 refers to $K = 0.2$ and Sc = 0.6, curve 2 to $K = -2$ and Sc = 0.6, and curve 3 to $K = 0.2$ and Sc = 0.16.

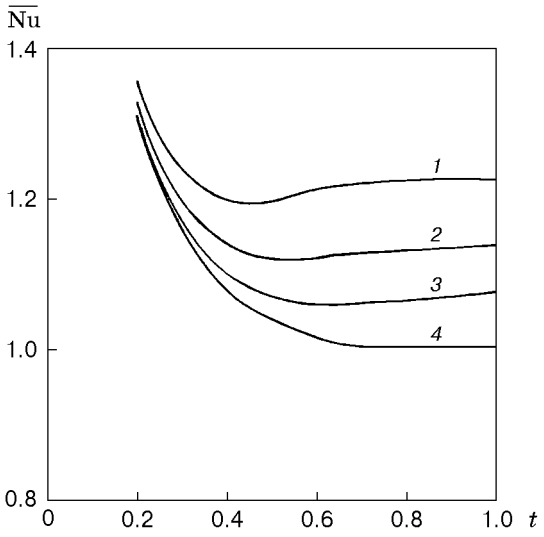

Fig. 11

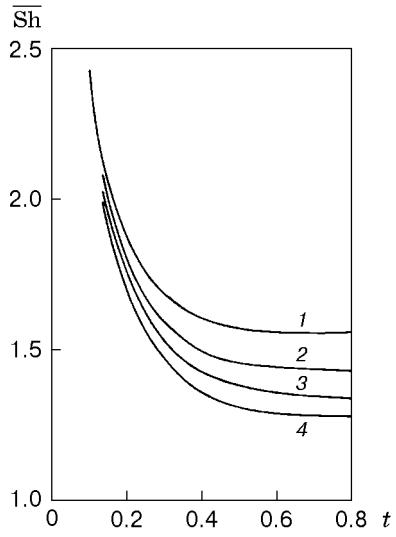

Fig. 12

Fig. 11. Averaged Nusselt number versus time (Pr = 0.71 and $K = 0.2$): curve 1 refers to Gr = 5, Gc = 10, and Sc = 0.6, curve 2 to Gr = 5, Gc = 5, and Sc = 0.6, curve 3 to Gr = 2, Gc = 5, and Sc = 0.6, and curve 4 to Gr = 2, Gc = 5, and Sc = 2.

Fig. 12. Averaged Sherwood number versus time (Gr = 2, Gc = 5, Sc = 0.6, and Pr = 0.71) for $K = 2$ (1), 0.2 (2), -1 (3), and -2 (4).

Knowing the velocity, temperature, and concentration fields, we can determine the skin friction, heat-transfer rate, and concentration rate in transient and steady regimes. The dimensionless and averaged values of skin friction and Nusselt and Sherwood numbers are determined by the following relations:

$$\tau_x = -\Big(\frac{\partial U}{\partial Y}\Big)_{Y=0}, \qquad \bar{\tau} = -\int\limits_0^1 \Big(\frac{\partial U}{\partial Y}\Big)_{Y=0} dX, \qquad \mathrm{Nu}_x = -X\Big(\frac{\partial T}{\partial Y}\Big)_{Y=0},$$

$$\overline{\mathrm{Nu}} = -\int\limits_0^1 \Big(\frac{\partial T}{\partial Y}\Big)_{Y=0} dX, \quad \mathrm{Sh}_x = -X\Big[\frac{(\partial C/\partial Y)_{Y=0}}{C_{Y=0}}\Big], \quad \overline{\mathrm{Sh}} = -\int\limits_0^1 \Big[\frac{(\partial C/\partial Y)_{Y=0}}{C_{Y=0}}\Big] dX. \tag{4}$$

We can estimate the derivatives entering system (4) using the five-point approximation formula and then calculate the integrals using the Newton–Cotes closed integration formula.

The local skin friction calculated by the first equation in (4) is plotted in Fig. 7 as a function of the axial coordinate X. The values of τ_x increase with increasing chemical reaction parameter or Schmidt number.

Figure 8 shows the dependence $\mathrm{Nu}_x(X)$. It is seen that the heat-transfer rate increases with increasing thermal and mass Grashof numbers and decreases with increasing Schmidt number. Figure 9 shows the dependence $\mathrm{Sh}_x(X)$. It is seen that the local Sherwood number increases with increasing Schmidt number. The concentration rate increases during the destructive reaction and decreases during the generative reaction.

The effect of Gr, Gc, Sc, and the chemical reaction parameter on the averaged values of skin friction and Nusselt and Sherwood numbers is shown in Figs. 10, 11, and 12. The mean value of skin friction increases with decreasing Gr or Gc and with increasing Sc during the entire transient period. The averaged Nusselt number increases with decreasing Sc and increasing Gr or Gc. The averaged Sherwood number increases as the chemical reaction parameter increases.

4. Conclusions. A detailed numerical study of the incompressible viscous fluid flow past an impulsively started semi-infinite isothermal vertical plate with homogeneous mass addition, taking into account the first-order homogeneous chemical reaction, is presented in the paper. Dimensionless equations are solved using the implicit finite-difference scheme of the Crank–Nicholson type. Air and water are considered here as a medium wherein the plate moves. The calculation results are in good agreement with the exact solution in the absence of the chemical reaction ($K = 0$). The study performed allows the following conclusions.

1. The velocity and concentration increase during the generative reaction ($K < 0$) and decrease during the destructive reaction ($K > 0$).

2. The temperature increases with increasing chemical reaction parameter and decreases with increasing Prandtl number.

3. The local and averaged values of the Sherwood number increase with increasing chemical reaction parameter.

REFERENCES

1. G. G. Stokes, "On the effect of internal friction of fluids on the motion of pendulums," *Cambridge Philos. Trans.*, **9**, 8–106 (1851).
2. V. M. Soundalgekar, "Free convection effects on the Stokes problem for an infinite vertical plate," *Trans. ASME, J. Heat Transfer*, **99**, 499–501 (1977).
3. V. M. Soundalgekar, "Effects of mass transfer and free convection currents on the flow past an impulsively started vertical plate," *Trans. ASME, J. Appl. Mech.*, **46**, 757–760 (1979).
4. R. Muthukumaraswamy and P. Ganesan, "Unsteady flow past an impulsively started vertical plate with heat and mass transfer," *Heat Mass Transfer*, **34**, 187–193 (1998).
5. U. N. Das, S. N. Ray, and V. M. Soundalgekar, "Mass transfer effects on flow past an impulsively started infinite vertical plate with constant mass flux — an exact solution," *Heat Mass Transfer*, **31**, 163–167 (1996).
6. U. N. Das, R. Deka, and V. M. Soundalgekar, "Effects of mass transfer on flow past an impulsively started infinite vertical plate with constant heat flux and chemical reaction," *Forsch. Ingenieurw.*, **60**, 284–287 (1994).
7. B. Carnahan, H. A. Luther, and J. O. Wilkes, *Applied Numerical Methods*, John Wiley and Sons, New York (1969).